Kinetic-energy release and fragment distribution of exploding, highly charged C_{60} molecules

S. Tomita, H. Lebius, A. Brenac, F. Chandezon, and B. A. Huber*
Département de Recherche Fondamentale sur la Matière Condensée (DRFMC), Groupe Ions Multicharges (GIM), CEA-Grenoble, 17 rue des Martyrs, 38054 Grenoble Cedex 9, France
(Received 10 December 2001; published 19 April 2002)

The kinetic-energy distributions of fragment ions formed in slow Xe^{25+}-C_{60} collisions have been determined with high-resolution time-of-flight mass spectrometry. The energy releases as well as the fragment size distributions are analyzed as functions of the number of electrons stabilized at the projectile, i.e., as a function of the average charge state of the intermediately formed C_{60} molecular ion. The evaluated energy releases are much higher than those reported for multiply charged ion collisions performed at high energies. The obtained results are consistent with the Coulomb explosion model, a fact which can be understood in terms of the high charge states involved.

DOI: 10.1103/PhysRevA.65.053201 PACS number(s): 36.40.Qv, 36.40.Wa, 34.70.+e

I. INTRODUCTION

The behavior of charged fullerene ions, in particular, the stability with respect to an excess of charge and the fragmentation processes occurring in the case of an instability have been studied with great effort during the last decade. The fullerene ions have been prepared either in collisions with neutral atoms [1], with electrons [2,3], with singly or multiply charged ions [4–12], or by irradiation with laser light [13–15]. Concerning the stability of C_{60} fullerenes, it has been shown that the molecule can survive on a μs-time scale up to charge states $r=10$ [16]. However, this value is very sensitive to the internal energy of the molecular ion, as has been recently demonstrated in the case of multiply charged sodium clusters [17]. Therefore, an increased effort has been made recently to analyze the energy deposit occurring during the collision, concentrating on the case of penetrating collisions of ions in low charge states [18–22]. Concerning the fragmentation processes, detailed information has been obtained for the thermally activated fission of fullerene ions in relatively low charge states ($r<9$) where asymmetric fission (emission of C_2^+ dimer ions) competes with the evaporation of neutral dimers [23–28]. However, for higher charge states the situation is more complex due to the large number of emitted fragments and similar detailed studies are still missing. On the other hand, recent experiments performing triple coincidence experiments, have clearly shown that processes with a high electron multiplicity, i.e., with a large number of active electrons do occur in collisions between highly charged ions and C_{60}. Thus, fullerene ions are created in very high charge states [29–31]. During the interaction, up to 100 electrons have been removed from the fullerene molecule, a similar phenomenon which occurs during the interaction of highly charged ions with surfaces [32,33]. However, the charge created within several femtoseconds stays within a defined volume in the case of the isolated C_{60} molecule and one might expect much more drastic effects due to the strong Coulomb repulsion and the corresponding high electric-field strengths.

In the present paper, we prepared the fullerene ions in such a type of collision ($Xe^{25+}+C_{60}$ at a collision energy of 280 keV). It is the aim to analyze the variation of the fragmentation pattern with the charge of the fullerene ion and to study the kinetic energy released during these processes. In the following, we will briefly describe the experimental setup before discussing the results concerning the fragment distributions and the involved energy releases.

II. EXPERIMENTAL SETUP

Projectile ions (Xe^{25+}) which are extracted from an electron cyclotron resonance ion source are accelerated to a final kinetic energy of 280 keV ($\nu=0.3$ a.u.). The ion beam crosses the effusive beam of C_{60} molecules at an angle of 90° inside the first stage of a Wiley-McLaren time-of-flight mass spectrometer. Due to the presence of an extraction field in the spectrometer, the ion beam needs an additional guiding by a steering plate system in order to pass the interaction zone. The C_{60} oven was operated at a temperature of about 500 °C.

After the collision, the projectile charge state is measured with an electrostatic energy filter consisting of two 90° spherical analyzers described in detail in Refs. [34,35]. Recoil ions and fragments are extracted with an electric-field strength of about 100 V/cm before entering a linear flight path of about 1 m in length. The time-of-flight measurement is started with the (charge-state analyzed) projectile ion detected after the collision and stopped with the recoil ion signal. Due to the electrostatic potential of the interaction zone, reactions inside the interaction zone are well separated from those occurring outside along the beam line. We used a time-to-digital converter which allows for multiple-stop detection, therefore several fragments stemming from one event could be detected and recorded. However, it should be noted, that due to dead time limitations of the detector and electronics (20 ns) the measured multiplicity (i.e., the number of charged fragments) is smaller than the real multiplicity. In addition the transmission through the spectrometer depends on the spectrometer setting and the kinetic energy of the fragments. This effect has been studied by performing trajectory calculations for the entire time-of-flight spectrometer with the SIMION program [36]. For each kinetic energy 5000 ion trajec-

*Email address: huber@ganil.fr

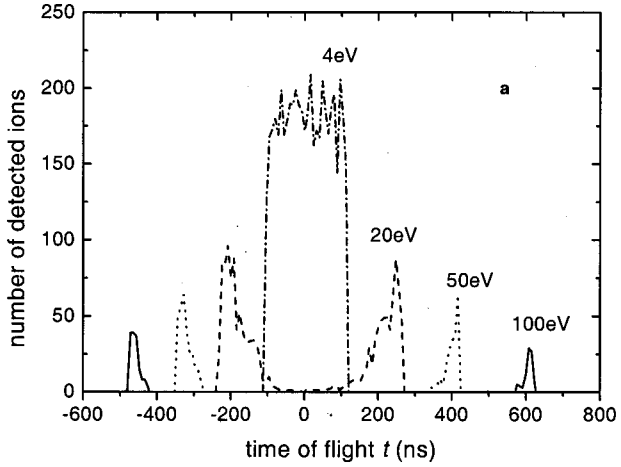

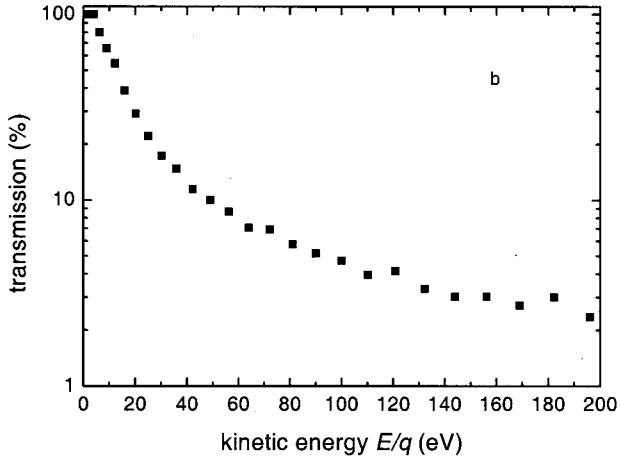

FIG. 1. (a) Simulated time-of-flight spectra for fragment ions characterized by different initial kinetic energies. $t=0$ corresponds to the time-of-flight of zero kinetic-energy fragments. (b) Variation of the spectrometer transmission function with the kinetic energy.

tories were calculated with the given initial energy and a distribution over the angles of the velocity vector (we assume that the emission is isotropic and does not depend on the initial direction of the projectiles). Since there are only electric fields in the time-of-flight (TOF) spectrometer, the spectrum shape depends only on the initial kinetic energy and not on the mass of the fragment. Typical time-of-flight distributions are shown in Fig. 1(a) for fragment ions with different kinetic energies (applying the chosen standard extraction voltages). Whereas for an energy of 4 eV all fragments are detected, producing a rectangular shape of the TOF peak, in the case of 100 eV only a small fraction arrives at the detector yielding a small ''forward'' and ''backward'' peak. In these cases the ions have been emitted parallel and antiparallel with respect to the detector direction. As can be seen in Fig. 1(b), for high fragment energies the transmission drops to values of a few percent approaching zero.

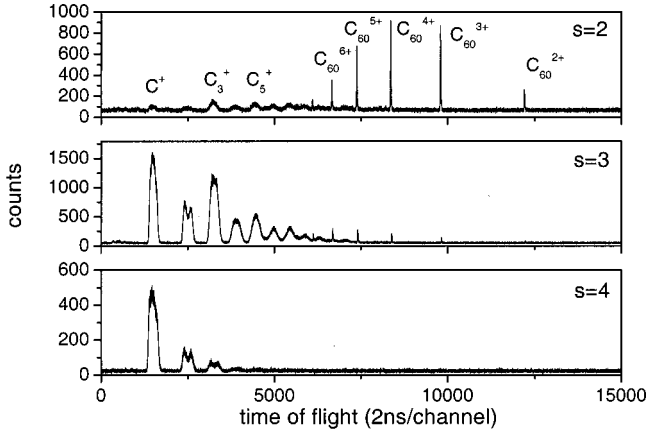

FIG. 2. Time-of-flight spectra of fragments produced in Xe^{25+}-C_{60} collisions for $2\cdots4$ stabilized electrons.

III. RESULTS AND DISCUSSION

In Fig. 2 the time-of-flight spectra of charged C_{60} ions and their fragments produced in the reaction

$$Xe^{25+} + C_{60} \rightarrow Xe^{(25-s)+} + C_{60}{}^{r+} + (r-s)e^- \qquad (1)$$

are shown for different values of stabilized electrons s. These spectra were measured by recording the time of flight of the recoil ions arriving in coincidence with a projectile ion with the charge $(25-s)$ after the collision. Two different kinds of product ions can be seen, charged intact fullerene ions $C_{60}{}^{q+}$ and small fragment ions $C_n{}^+$. For $s=2$ the spectrum shows large contributions from nondissociated, multiply charged $C_{60}{}^{q+}$ ions. For $s=3$, their contribution becomes negligible with respect to the intensity of small singly charged carbon clusters (C_n^+). For $s=4$, only very small fragments are detected. The width of the fullerene ion peaks is very small, whereas it is broad for the fragment ion peaks. This is explained by the fact, that fragment ions produced during the decay of the intermediately formed highly charged fullerene ion receive large kinetic energies due to the electrostatic repulsion. The intact fullerene ions have only a low thermal energy as nearly no momentum is transferred at large impact parameters. When more electrons are stabilized ($s>4$), the major contribution to the time-of-flight spectrum is due to atomic C^+ ions, indicating the total destruction of the fullerene cage. In addition multiply charged atomic ions in charge states up to $q=4$ are detected.

As can be seen in Fig. 2 for $s=4$ and to a less extent for $s=3$, the peak form of the fragments $C_2{}^+$ and $C_3{}^+$ shows two maxima, whereas this is not the case for the C^+ fragments. This becomes more clear in Fig. 3, where the time-of-flight region of the atomic fractions C^+ and C^{2+} is shown for the case of seven stabilized electrons. The C^{2+} distribution consists of two distinct peaks, representing ions ejected towards and away from the detection system. The turn-around time of the ''backward'' ions in the extraction field is the time difference between the two peaks. Both peaks are of different height due to the different acceptance angles for ''forward'' and ''backward''-emitted fragments of equal en-

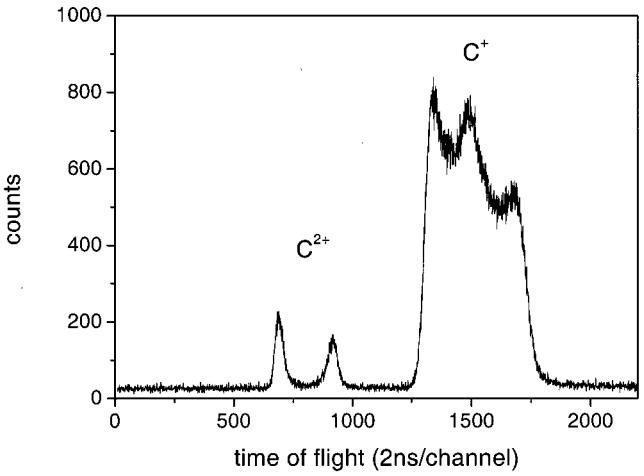

FIG. 3. Time-of-flight spectrum of C^+ and C^{2+} fragments produced in Xe^{25+}-C_{60} collisions for seven stabilized electrons.

ergy [see simulations in Fig. 1(a) for high kinetic energies]. Surprisingly, the C^+ distribution shows a third, central peak at the position which corresponds to C^+ ions with low kinetic energy.

In order to determine the initial kinetic-energy distributions of the recoil ions, the measured time distributions $F(t)$ have been fitted with a linear combination of the simulated TOF-spectra $f(\varepsilon_k,t)$

$$F(t)=\Sigma w_k f(\varepsilon_k,t), \tag{2}$$

where

$$\varepsilon_k=(0.5\ \mathrm{k})^2\mathrm{eV} \tag{3}$$

represents the fragment kinetic energy varying from 0.25 eV up to 196 eV.

The resulting kinetic-energy distributions for C^+ and C^{2+} fragments are shown in Fig. 4 for $s=5$ and 11.

In the case of doubly charged C atoms the kinetic energy is well defined, increasing from about 90 eV for $s=5$ to about 180 eV for $s=11$. This finding can be understood easily as an increasing number s of stabilized electrons also means an increasing number r of electrons captured from the target. According to Refs. [30,31] the charge state of the intermediately formed C_{60}-ion increases from 20 to 50. Therefore, the potential energy which is transferred into kinetic energy of the fragments during the Coulomb explosion increases as well.

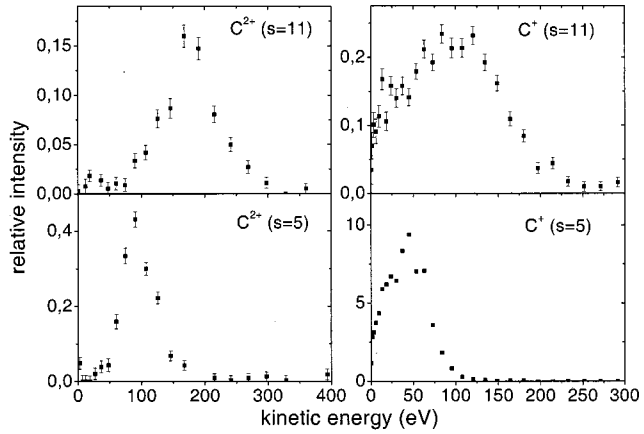

FIG. 4. Kinetic-energy spectra for C^+ and C^{2+} ions for 5 and 11 stabilized electrons. The measured time-of-flight spectra have been deconvoluted and corrected for the transmission function.

The situation is more complex in the case of C^+ fragments. As was already evident in Fig. 3, a high-energy part exists which shifts from 45 eV to about 100 eV when s is increased from 5 to 11. These energies are approximately a factor of 2 smaller than those of the C^{2+} fragments. However, there are considerable contributions from C^+ ions with very low kinetic energies, at around 20 eV. These contributions do not exist for C^{2+} ions and they do not depend on s and hence on the charge state of the fullerene ion. The fact, that these fragments do not take part in the Coulomb acceleration of the decaying highly charged fullerene, might be expected when the carbon fragment is inside the fullerene sphere during the expansion of the molecular ion. We assume that in a tangential collision with the projectile one of the carbon atoms is pushed inside the cage with an energy transfer of several electron volts. An estimation of the time evolution of the system shows, that the projectile has left before the Coulomb explosion of the molecule evolves. Furthermore, the expansion of the cage proceeds so fast, that a carbon atom with 10 or 20 eV will stay inside the exploding system. When the energy transferred to the atom is larger, it will not be detected in the spectrometer as it will miss the acceptance angle. The fact that this phenomenon shows up for C^+ ions only might be plausible, as the charge tries to distribute itself on the outside of the cage. It is unlikely, that the C ion inside keeps a higher charge state than one. In many cases it might even be neutral and thus escapes the detection system. Further experimental evidence is needed to understand the origin of these low-energy C^+ ions and to verify the proposed mechanism.

Triply and four times charged atomic fragments, which are probably due to reactions with $s>11$ and which have been analyzed for intensity reasons only in the inclusive spectrum (no correlation with s), are formed with much higher kinetic energies. The most probable energies are 200 and 300 eV, with energetic tails going up as high as 500 and 800 eV, respectively. As will be discussed later, these high kinetic energies require a fullerene charge state of 80 or 100 in order to be explained by a Coulomb explosion model.

For small values of s ($s<7$), multiply charged Carbon ions are not detected, however, singly charged, molecular fragments are measured. As can be seen in Fig. 2, these molecular fragments are formed with high probability for $s=3$. The kinetic-energy distributions for C_n^+ fragments, $n=1$ to 8, are shown in Fig. 5 for this case. In general, the most likely kinetic energy decreases with the size of the fragment, changing from 20 eV for C^+ ions to 3 eV for C_8^+.

According to Refs. [30,31], $s=3$ is linked to a range of active electrons between 10 and 20, with a maximum probability at $r=15$. From the variation with s we conclude that

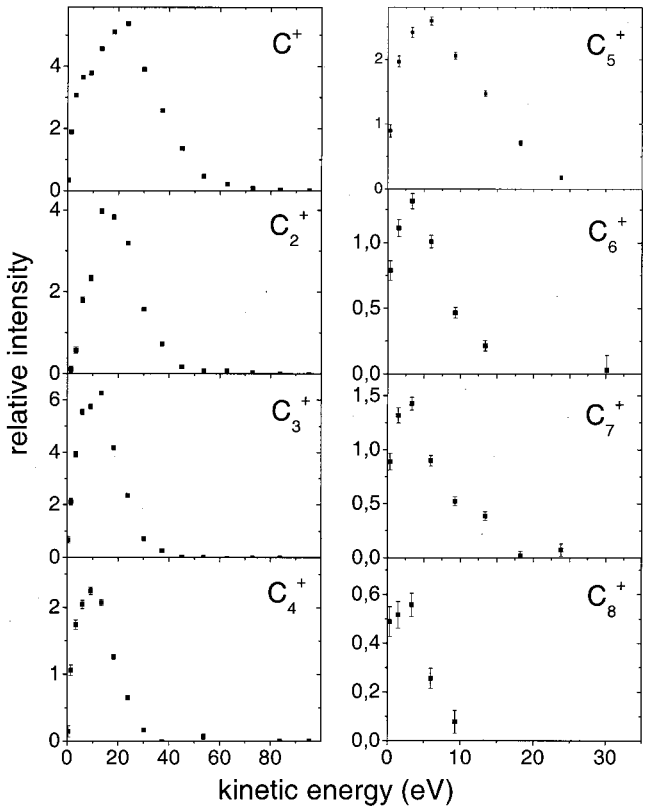

FIG. 5. Kinetic-energy spectra for molecules C_n^+, $n=1\cdots8$, when three electrons have been stabilized.

larger fragments are formed when the charge is small, and smaller fragments are emitted when the charge of the fullerene ion is high.

In order to summarize the observed results, we have determined from the energy distributions, as shown in Figs. 4 and 5, an average kinetic fragment energy. The result is shown in Fig. 6 as a function of the fragment size and the number of stabilized electrons *s*. One observes a clear decrease with increasing size (close to an exponential dependence) and an increase with *s*, i.e., with the charge state of the decaying fullerene ion.

Similar results have been published for collisions of ions in low charge states (<5) colliding with C_{60} at MeV-energies [37,38]. In contrast to the present results, the energy distributions of the fragment ions always peak at zero energy and the average energies decrease from 6 to 0.8 eV when the fragment size is increased from 1 to 12. In these systems the involved charge states are much lower and multifragmentation processes are explained by strong excitations occurring in penetrating collisions, i.e., as thermally activated decay processes. In the present case, we believe that charge instabilities are the main source for provoking the fragmentation process.

The relative yields of small fragments are shown in Fig. 7(a) as a function of the fragment size. The fragment distributions show even-odd oscillations which are well known from the decay of metal clusters [see Fig. 7(b)] and which are based on the different stability or binding energy of clusters containing an even or odd number of constituents or electrons, respectively. In general, the intensity decreases with increasing fragment size, thus C^+ is the most important fragment, except for $s=2$, where the trimer is dominant. When *s* is increased, the intensity declines much faster towards larger fragment sizes and for $s>7$ only atomic fragments in different charge states are detected. A quite similar tendency is found in the case of highly charged sodium clusters, shown in Fig. 7(b). In this case sodium clusters with an average size of 200 are ionized in collisions with Xe^{18+} ions. Whereas for $s=2$ the trimer is the most abundant fragment, it is the monomer for higher *s* values. The observed similarity between sodium clusters and fullerenes indicates that the decrease of the fragment size with increasing charge of the system is a rather general characteristic of charge-induced instabilities of complex systems.

In order to quantify the initial charge state of the interme-

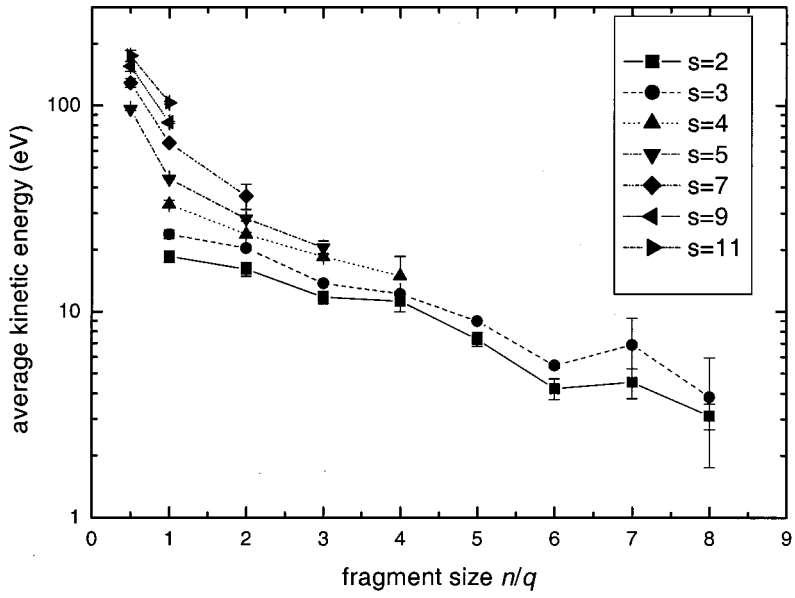

FIG. 6. Average kinetic energy as a function of the size of the fragment ion.

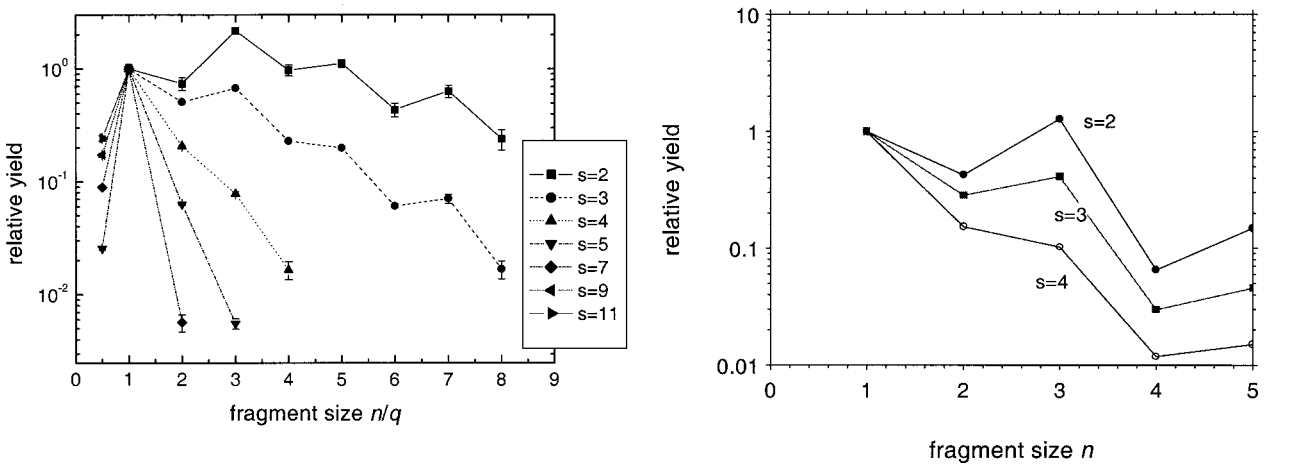

FIG. 7. Relative intensity of fragment ions corrected for the energy-dependent acceptance angle of the spectrometer. Left part: fragment distribution after Xe^{30+}-C_{60} collisions; right part: fragment distributions after Xe^{18+}-Na_n collisions ($n \sim 200$).

diately formed fullerene ion, we approximate the charged fullerene cage by a charged conducting sphere. The total electrostatic potential-energy E_{tot} of the system is given by

$$E_{\mathrm{tot}} = {Q_{\mathrm{tot}}}^2/2R, \tag{4}$$

where Q_{tot} denotes the total charge and R the radius of the sphere. This can be rewritten in the following form:

$$Q_{\mathrm{tot}} = 2R/(Q_{\mathrm{tot}}/E_{\mathrm{tot}}). \tag{5}$$

When we assume, that the electrostatic energy of the charged sphere is totally converted into the kinetic energy of the charged fragments and when we neglect the binding energy needed to fragment the fullerene cage, we can write the following expressions for Q_{tot} and E_{tot}:

$$Q_{\mathrm{tot}} = \alpha \Sigma q_i Y_i / N \tag{6}$$

and

$$E_{\mathrm{tot}} = \alpha \Sigma \langle E \rangle_i Y_i / N. \tag{7}$$

Here, $\langle E \rangle_i$ is the average kinetic energy of the ith fragment (see Fig. 6), Y_i its yield, and N the number of events contributing to the spectrum measured for a given s. The detection efficiency α is assumed to be independent of the fragment size. In order to avoid ambiguities in α and N we consider the ratio $(Q_{\mathrm{tot}}/E_{\mathrm{tot}})$

$$Q_{\mathrm{tot}}/E_{\mathrm{tot}} = \Sigma q_i Y_i / \Sigma \langle E \rangle_i Y_i . \tag{8}$$

Together with Eq. (5) we obtain the charge of the decaying fullerene ion as a function of s, shown in Fig. 8. A remarkably good agreement between the determined charge state and the number of active electrons measured by Martin *et al.* [30] and Bredy [31] is found. From this comparison we conclude that the main assumptions in the analysis are confirmed: (i) The charge is equally distributed on the fullerene sphere, (ii) the radius of the fullerene cage stays constant during the presence of the projectile, and (iii) especially for higher charge states, the decay can be described well within the model of a Coulomb explosion.

The energetic balance of the process where the fullerene loses 50 electrons, out of which 11 are stabilized at the projectile, shows that a large amount of potential energy is involved in the reaction. The energy necessary to ionize the fullerene 50 times equals the electrostatic energy E_{tot} and is of the order of 4.8 keV (neglecting the expansion of the fullerene cage during the capture process). The energy which can be gained by the recombination of 11 electrons can be calculated with a Dirac-Fock code [39]. It is of the order of 6.3 keV when capture occurs into the ground state. Thus, the difference of 1.5 keV has to be distributed among the excitation energy of the Xe^{14+} ion, the kinetic energy of the emitted electrons, and the energy gain of the projectile. As the projectile is measured as a stable system on a μs time scale it is likely that the excitation energy is lower or equal to the ionization potential of Xe^{14+} (344 eV). The measured

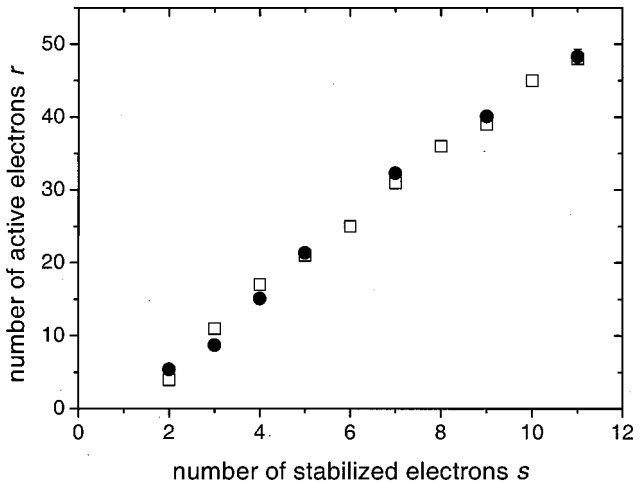

FIG. 8. Charge state Q_{tot} of the fullerene ion (equals number of active electrons) as a function of the number s of stabilized electrons. Full circles: present result; open rectangles: Martin *et al.* [30] and Bredy [31].

energy gain of the projectile is close to zero. Therefore, the larger part of the energy difference has to be found in the kinetic energy of the emitted electrons, yielding an average value of ~30 eV per electron.

IV. SUMMARY

The fragmentation pattern of highly charged C_{60} fullerene ions, produced in the interaction of Xe^{25+} ions with neutral C_{60} molecules, has been analyzed as a function of the fullerene charge state r. The analysis of the fragmentation spectra measured in correlation with the number of electrons stabilized by the projectile ion shows that the fragment size decreases strongly when the charge is increased. For $s>7$ (corresponding to $r>30$) only monoatomic fragments are detected in charge states varying from 1 to 4. On the other hand, the fragment kinetic energies increase strongly with decreasing fragment size and increasing fullerene charge, yielding in the extreme cases kinetic energies of the order of several hundreds of electron volts. The fact that low-energy C^+ fragments are measured in correlation with high charge states of the fullerene ion ($s=11$ or $r=\sim 50$) is surprising, but might be a consequence of the hollow sphere structure of the fullerene which allows ions inside the sphere not to participate in the Coulomb repulsion in the early stage of the explosion.

The average number of active electrons was deduced by equating the electrostatic energy of a charged sphere with the total kinetic-energy release of the fragments. The surprisingly good agreement of the obtained values with those being measured in another experiment [29] indicates that at least for higher charges the Coulomb explosion model is capable to describe the coarse features of the fragmentation process.

It should be noted that the present analysis discusses mainly average properties and the dominant decay mechanisms. Specific processes like the evaporation of dimers is not included. However, we believe that in the present collision system the influence is relatively small, as for large values of s the produced fullerene charge is always favoring fission processes. For small s values the collisions are characterized by large-impact parameters where the energy transfer is rather small. Reaction products of penetrating collisions, connected with a large energy loss of the projectile ion, do not contribute to the presented spectra. According to Ref. [31], these processes are linked to even larger values of stabilized electrons ($s>13$).

ACKNOWLEDGMENTS

The experiments have been performed at the Accélérateur d'Ions Multichargés a facility of CEA-Grenoble. The authors would like to thank F. Gustavo and X. Biquard for preparing the ion beam.

[1] E. E. B. Campbell, T. Raz, and R. D. Levine, Chem. Phys. Lett. **253**, 261 (1996).
[2] S. Matt, O. Echt, R. Wörgötter, V. Grill, P. Scheier, C. Lifschitz, and T. D. Märk, Chem. Phys. Lett. **264**, 149 (1997).
[3] A. Itoh, H. Tschuchida, T. Majima, and N. Imanishi, J. Phys. B **32**, 277 (1999).
[4] T. LeBrun, H. G. Berry, S. Cheng, R. W. Dunford, H. Esbensen, D. S. Gemmell, and E. P. Kanter, Phys. Rev. Lett. **72**, 3965 (1994).
[5] B. Walch, C. L. Cocke, R. Voelpel, and E. Salzborn, Phys. Rev. Lett. **72**, 1439 (1994).
[6] Jian Jin, H. Khemliche, M. H. Prior, and Z. Xie, Phys. Rev. A **53**, 615 (1996).
[7] N. Selberg, A. Barany, C. Biedermann, C. J. Setterlind, H. Cederquist, A. Langereis, M. O. Larsson, A. Wännström, and P. Hvelplund, Phys. Rev. A **53**, 874 (1996).
[8] A. Itoh, H. Tschuchida, T. Majima, and N. Imanishi, Phys. Rev. A **59**, 4428 (1999).
[9] T. Miura, I. Arai, M. Imanaka, H. Sasaki, S. Tomita, and S. M. Lee, Phys. Rev. A **62**, 021201(R) (2000).
[10] H. Cederquist, A. Fardi, K. Haghighat, A. Langereis, H. T. Schmidt, S. H. Schwartz, J. C. Levin, I. A. Sellin, H. Lebius, B. A. Huber, M. O. Larsson, and P. Hvelplund, Phys. Rev. A **61**, 022712 (2000).
[11] A. Bordenave-Montesquieu, P. Moretto-Capelle, D. Bordenave-Montesquieu, H. Lebius, and B. A. Huber, J. Phys. B **33**, L357 (2000).
[12] S. Martin, L. Chen, A. Denis, and J. Désesquelles, Phys. Rev. A **57**, 4518 (1998).
[13] N. Hay, E. Springate, M. B. Mason, J. W. G. Tisch, M. Castillejo, and J. P. Marangos, J. Phys. B **32**, L17 (1999).
[14] R. C. Constantinescu, S. Hunsche, H. B. van Linden van den Heuvell, and H. G. Müler, Phys. Rev. A **58**, 4637 (1998).
[15] J. Kou, V. Zhakovskii, S. Sakabe, K. Nishihara, S. Shimizu, S. Kawato, M. Hashida, K. Shimuzu, S. Bulanov, Y. Izawa, Y. Kato, and N. Nakashima, J. Chem. Phys. **112**, 5012 (2000).
[16] A. Brenac, F. Chandezon, H. Lebius, A. Pesnelle, S. Tomita, and B. A. Huber, Phys. Scr., T **80**, 195 (1999).
[17] F. Chandezon, S. Tomita, D. Cormier, P. Grübling, C. Guet, H. Lebius, A. Pesnelle, and B. A. Huber, Phys. Rev. Lett. **87**, 153402 (2001).
[18] J. Opitz, H. Lebius, S. Tomita, B. A. Huber, P. Moretto-Capelle, D. Bordenave-Montesquieu, A. Bordenave-Montesquieu, A. Reinköster, U. Werner, H. O. Lutz, A. Niehaus, M. Benndorf, K. Haghighat, H. T. Schmidt, and H. Cederquist, Phys. Rev. A **62**, 022705 (2000).
[19] T. Schlathölter, O. Hadjar, R. Hoekstra, and R. Morgenstern, Phys. Rev. Lett. **82**, 73 (1999).
[20] O. Hadjar, P. Földi, R. Hoekstra, R. Morgenstern, and T. Schlathölter, Phys. Rev. Lett. **84**, 4076 (2000).
[21] D. Bordenave-Montesquieu, P. Moretto-Capelle, A. Bordenave-Montesquieu, and A. Rentenier, J. Phys. B **34**, L137 (2001).
[22] T. Kunert and R. Schmidt, Phys. Rev. Lett. **86**, 5258 (2001).
[23] P. Scheier, B. Dünser, R. Wörgötter, D. Muigg, S. Matt, O. Echt, M. Foltin, and T. D. Märk, Phys. Rev. Lett. **77**, 2654 (1996).

[24] B. Dünser, O. Echt, P. Scheier, and T. D. Märk, Phys. Rev. Lett. **79**, 3861 (1997).

[25] J. Opitz and B. A. Huber, in *Similarities and Differences between Atomic Nuclei and Clusters*, edited by Y. Abe, I. Irai, S. M. Lee, and K. Yabana, AIP Conf. Proc. No. 416 (AIP, Woodbury, NY, 1998), p. 422.

[26] H. Lebius, S. Tomita, A. Brenac, F. Chandezon, A. Pesnelle, and B. A. Huber, Phys. Scr., T **80**, 197 (1999).

[27] S. Martin, L. Chen, A. Denis, R. Bredy, J. Bernard, and J. Désesquelles, Phys. Rev. A **62**, 022707 (2000).

[28] L. Chen, S. Martin, R. Bredy, J. Bernard, and J. Désesquelles, Phys. Rev. A **64**, 031201(R) (2001).

[29] S. Martin, J. Bernard, L. Chen, A. Denis, and J. Désesquelles, Eur. Phys. J. D **12**, 27 (2000).

[30] S. Martin, L. Chen, A. Denis, and J. Désesquelles, Phys. Rev. A **59**, R1734 (1999).

[31] R. Bredy, Ph.D. thesis, Université ClaudeBernard, Lyon I, France, 2001.

[32] F. Aumayr, H. Kurz, D. Schneider, M. A. Briere, J. W. McDonald, C. E. Cunningham, and H.P. Winter, Phys. Rev. Lett. **71**, 1943 (1993).

[33] H. Kurz, F. Aumayr, HP. Winter, D. Schneider, M. A. Briere, and J. W. McDonald, Phys. Rev. A **49**, 4693 (1994).

[34] T. Bergen, X. Biquard, A. Brenac, F. Chandezon, B. A. Huber, D. Jalabert, H. Lebius, M. Maurel, E. Monnand, J. Opitz, A. Pesnelle, B. Pras, C. Ristori, and J. C. Rocco, Rev. Sci. Instrum. **70**, 3244 (1999).

[35] A. Pesnelle and H. J. Andrä, Rev. Sci. Instrum. **68**, 3702 (1997).

[36] D. A. Dahl, J. E. Delmore, and A. D. Appelhans, Rev. Sci. Instrum. **61**, 607 (1990).

[37] A. Itoh, H. Tsuchida, K. Miyabe, M. Imai, and N. Imanishi, Nucl. Instrum. Methods Phys. Res. B **129**, 363 (1997).

[38] H. Tsuchida, A. Itoh, K. Miyabe, Y. Bitoh, and N. Imanishi, J. Phys. B **32**, 5289 (1999).

[39] J. P. Desclaux, Comput. Phys. Commun. **9**, 31 (1975); and data-base, Plasma relevant atomic data, established by B. Fricke, H. J. Blanke, D. Heinemann, and W. Eckstein (1991).